Adsorption Characteristics of Arylisocyanide on Au and Pt Electrode Surfaces: Surface-Enhanced Raman Scattering Study

Nam Hoon Kim and Kwan Kim*

Laboratory of Intelligent Interfaces, School of Chemistry, Seoul National University, Seoul 151-742, Korea

Received: September 29, 2005; In Final Form: December 9, 2005

It is very important to understand metal−molecule interface characteristics for the development of efficient molecular wires in molecular electronics. Because isocyanide is potentially a good alligator clip, we have investigated in this work the adsorption characteristics of 2,6-dimethylphenylisocyanide (DMPI) on Au and Pt electrodes by recording the potential-dependent surface-enhanced Raman scattering (SERS) spectra. First of all, we confirmed that Pt nanoaggregate films were efficient SERS-active substrates, not only in ambient conditions, but also in electrochemical environments. Second, we confirmed that aryl isocyanide should adsorb on Au and Pt by forming exclusively metal−CN bonds, via a pure σ type interaction in the case of gold compared with a σ/π synergistic interaction on Pt. This implies that DMPI should adsorb on Au only via the on-top site, whereas not only the on-top site, but also the 2-fold bridge and 3-fold hollow sites, could be used in the surface adsorption of DMPI on Pt. Despite these differences, DMPI was assumed to possess a vertical orientation with respect to the Au and Pt substrates, irrespective of the potential variation between +0.2 and −0.6 V relative to the Ag/AgCl reference electrode. The latter characteristics of the Au−CN and Pt−CN combinations are presumed to be useful in designing molecular-scale wires.

1. Introduction

Observation of the vibrational spectra of adsorbed molecules is one of the most incisive methods to understand chemical and physical phenomena occurring at metal electrode surfaces. In this light, subtractively normalized interfacial Fourier transform infrared spectroscopy (SNIFTIRS)[1] as well as polarization-modulated infrared reflection−absorption spectroscopy (PMIRAS)[2] has successfully been applied to numerous electrochemical systems. Unfortunately, however, because of the intrinsic properties of infrared radiation, the spectral data at low wavenumber (<800 cm^{-1}) can hardly be obtained by SNIFTIRS and PMIRAS. In addition, very flat metal electrodes have to be employed in such infrared studies. These difficulties can be overcome by adopting Raman spectroscopy, but the Raman process itself is inherently weak. Nonetheless, Raman spectra can be readily acquired on rough noble metal electrodes, such as Ag, Au, and Cu, owing to the surface-enhanced Raman scattering (SERS) effect.[3,4] In an effort to extend SERS to other important materials such as transition metals such as Pt, ultrathin films, normally with 3−10 atomic layers, have been deposited onto the SERS-active substrate by Weaver et al.[5] Tian and his colleagues reported that transition metals could be made to be SERS-active via several roughening processes.[6] Recently, we were able to record SERS spectra, even with visible excitation, for organic monolayers assembled on Pt nanoparticles, specifically those with diameters greater than 15 nm.[7]

Molecular electronics has been an active research area in recent years, leading to the design and synthesis of very diverse organic molecular devices (such as wires, switches, rectifiers, storages, transistors, and so on).[8,9] There have been several theoretical[10,11] and experimental[12] attempts to determine the best combination of metal−molecule interfaces, but unequivocal conclusions have not yet been reached. By comparing the conductance of different terminal atom−electrode metal combinations, Yaliraki et al.[13] reported that the conductance should be larger when the wire is terminated by selenium rather than by sulfur or oxygen. They also claimed that gold should be a better electrode than silver. According to theoretical analyses of Seminario et al.,[10] the order of increasing quality of metals for the metal−molecule interface appeared to be Pd, Ni, Pt, Cu, and Au and Ag. The best atom to be bonded to metal was predicted to be S, but it seemed not to be much better than CN. Besides the conductance data, it is also important to understand the molecule−metal adsorption characteristics for the fabrication of stable, effective, and reproducible individual, or small, packets of molecular electronic devices. In this respect, it is noteworthy that the adsorption characteristics of aliphatic, as well as aromatic, thiols on gold have been extensively studied by microscopic and spectroscopic tools, but relatively little is known about the adsorption nature of isocyanides on Au. It has been reported that M−CN bonds are readily formed when isocyanides are adsorbed on Au, as well as on Ag, Cr, Co, Pt, Pd, and Ru.[14−26] Nonetheless, surface vibrational spectral data are very limited for isocyanides, particularly in electrochemical environments.

In conjunction with above implications, the adsorption and interface characteristics of 2,6-dimethylphenylisocyanide (DMPI) at Pt and Au electrodes have been investigated in this work by recording the potential-dependent SERS spectra. DMPI was confirmed to bind to Au and Pt electrodes by forming Au−C and Pt−C bonds. The detailed adsorption characteristics were, however, significantly different for the two cases. Three different NC stretching bands were identified on a Pt electrode, while only one NC stretching band was observed on an Au electrode. The appearance of a single NC stretching band indicated that the bonding to Au occurred merely via a σ type interaction. On the other hand, the observation of three different NC stretching

* To whom all correspondence should be addressed. E-mail: kwankim@snu.ac.kr. Telephone: +82-2-8806651. Fax: +82-2-8891568.

10.1021/jp055541v CCC: $33.50
Published on Web 01/07/2006

bands suggested that a σ/π synergistic interaction should be involved when DMPI was adsorbing on a Pt electrode. Those three bands could be attributed to DMPI adsorbed at three different bonding sites of a Pt electrode surface, namely a three-atom hollow site, a two-atom bridge site, and a single-atom on-top site, with the metal-to-adsorbate π back-bonding occurring most extensively at the three-atom hollow site. This paper is unique in that we could identify, solely by SERS, the presence of three different adsorption sites on Pt in an electrochemical environment. The potential-dependent SERS spectra indicated that the molecular orientation of DMPI on Au and Pt was not subjected to change by the variation of the electrode potential, and such interface characteristics should be helpful when designing molecular electronics circuits.

2. Experimental Section

2,6-Dimethylphenylisocyanide (DMPI) was purchased from Fluka and used as received. Au (99.99%) and Pt (99.99%) were purchased from Aldrich. All other chemicals were of reagent grade, unless specified otherwise, and ultrapure water, of resistivity >18.0 MΩ·cm (Millipore Milli-Q system), was used to prepare aqueous solutions. As in the previous work, Au[27] and Pt[28] nanoparticles were obtained via laser ablation using radiation of 1064 nm excitation from a Continuum Surelite II-10 Nd:YAG laser with 100 mJ pulse energy, 10 Hz repetition rate, and 6 ns laser pulse duration.

Au and Pt nanoaggregate films were prepared by dropping 15 μL of Au and Pt sol solutions onto macroscopically smooth, polycrystalline Au and Pt substrates, respectively.[28] The injected substrates were left to dry under ambient conditions to form uniform and circular nanoaggregate films. The films were washed again with triply distilled water and then dried under N_2 atmosphere. The initial Au and Pt substrates that had been polished to a mirror finish were SERS-inactive, but they became SERS-active by deposition of Au and Pt nanoaggregates thereon.

Raman spectra were obtained by using a Renishaw Raman system model 2000 spectrometer equipped with an integral microscope (Olympus BH2-UMA). The 632.8-nm line from a 17-mW He/Ne laser (Spectra Physics model 127) was used as the excitation source, and Raman scattering was detected over 180° by using a Peltier-cooled (−70 °C) charge-coupled device (CCD) camera (400 × 600 pixels). The holographic grating (1800 grooves/mm) and the slit allowed the spectral resolution to be 1 cm^{-1}. The Raman band of a silicon wafer at 520 cm^{-1} was used to calibrate the spectrometer, and the accuracy of the spectral measurement was estimated to be better than 1 cm^{-1}. The Raman spectrometer was interfaced with an IBM-compatible PC, and the spectral data were analyzed with Renishaw WiRE software v. 1.2 based on the GRAMS/32C suite program (Galactic). The potential of the electrochemical cell used for Raman spectral measurement was controlled by using a CH Instruments model 660A potentiostat, which employed CHI 660A electrochemical analyzer software (version 2.03) running on an IBM-compatible PC. All potentials are reported with respect to the Ag/AgCl electrode.

UV−visible spectra of Au and Pt sols were recorded on a SCINCO S-2130 spectrophotometer. TEM images of Au and Pt nanoparticles were acquired by using a JEM-200CX transmission electron microscope at 160 kV after dropping Au and Pt sols onto carbon-coated copper grids (150 mesh). AFM images of Au and Pt nanoaggregate films were obtained with a Digital Instruments model Nanoscope IIIa scanning probe microscope. Specifically, by using a V-shaped, 200-μm-long Si_3N_4 cantilever with a nominal spring constant of 0.12 N/m (Nanoprobe, Digital Instruments), topographic images were recorded in the conventional height mode (tapping mode, normal AFM) at a scan rate of 2−5 Hz.

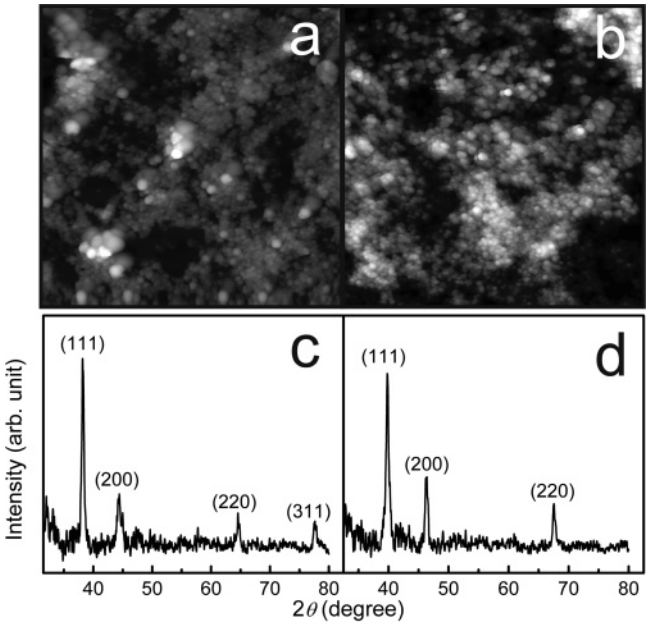

Figure 1. Tapping-mode AFM images (2 μm × 2 μm) of (a) Au and (b) Pt nanoaggregates assembled on macroscopically smooth Au and Pt substrates, respectively. X-ray diffractograms of (c) Au and (d) Pt nanoaggregates assembled on glass slides.

3. Results and Discussion

Morphological Features of Au and Pt Nanoaggregate Films. Initially, Au and Pt nanoparticles were prepared by laser ablation simply on the grounds that laser ablation is rapid and simple, and that it produces metal colloids with highly reproducible properties. According to the TEM measurements, the average diameters of >500 Au and Pt particles in the as-prepared state were ∼15 and ∼8 nm, respectively. The size distribution of Au particles was smooth and narrow, but for Pt sol, tiny Pt particles smaller than 2 nm were prevalent in the sol. There were also Pt nanoparticles larger than 15 nm that were found recently to be effective for SERS.[7,28] As reported previously, the smaller Pt nanoparticles were removed by repeated centrifugation cycles at 3000 rpm. The average size of the Pt nanoparticles thus obtained was ∼17 nm and they were of highly spherical shape. As also reported previously, in the UV−vis spectrum of Pt sol, there was no characteristic peak in the region of 300−800 nm, and only a gradual increase in absorption toward the blue was identified. A highly distinct surface-plasmon band could be seen at ∼520 nm, however, in the UV−vis spectrum of Au sol (data not shown).

As described in the Experimental Section, Au and Pt nanoaggregate films were fabricated by dropping 15 μL of Au and Pt sol solutions onto macroscopically smooth, polycrystalline Au and Pt substrates, respectively. Parts a and b of Figure 1 show the tapping mode AFM images of these Au and Pt nanoaggregates assembled on Au and Pt electrodes, respectively. Their morphologies are seen to be very rough and complicated. The heights of Au and Pt nanoparticles were measured to be about 20 nm, in good agreement with the sizes of nanoparticles determined from the TEM images. The root-mean-square roughness values estimated from 10 different measurements were also ∼20 nm for both the Au and Pt nanoaggregate films. In parts c and d of Figure 1 are shown the X-ray diffractograms

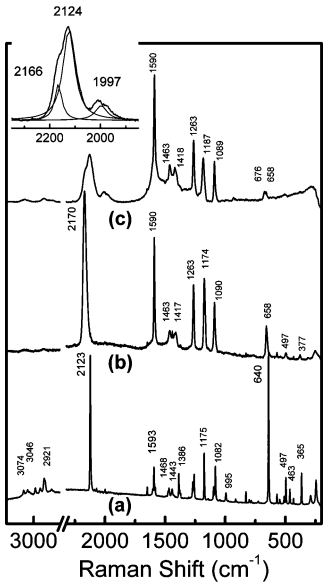

Figure 2. (a) NR spectrum of DMPI in neat state. SERS spectra of DMPI adsorbed on (b) Au and (c) Pt nanoaggregate films assembled, respectively, on macroscopically smooth Au and Pt substrates. All the spectra herein were obtained by using a He/Ne laser at 632.8 nm as the excitation source. The inset shows the intensity ratio of the three NC stretching peaks at 2166, 2124, and 1997 cm^{-1} in (c) to be ~3:14:1.

(XRDs) of Au and Pt nanoaggregate films that have been fabricated by dropping 15 μL of Au and Pt sol solutions onto glass slides. By analyzing the bandwidths of the XRD peaks, the sizes of Au and Pt nanoparticles were determined to be 17.5 and 16.2 nm, respectively.

Binding Characteristics of DMPI on Au and Pt. To obtain Raman spectra of DMPI adsorbed on Au and Pt surfaces, the Au and Pt nanoaggregate films mentioned above were dipped in 1 mM DMPI ethanol solution for 6 h and then washed with ethanol and triply distilled water, followed by drying in N_2 atmosphere. Parts b and c of Figure 2 show the Raman spectra of DMPI thus prepared on Au and Pt nanoaggregate films, respectively. For comparison, the normal Raman (NR) spectrum of neat DMPI powder is shown in Figure 2a. The two intense peaks at 2123 and 640 cm^{-1} in Figure 2a are due to the NC stretching and C−NC stretching vibration, respectively.[29] Ring-associated bands are comparatively less intense than the NC associated bands, as can be evidenced from the peaks at 3046, 1593, and 995 cm^{-1} in Figure 2a that can be assigned to the CH stretching, the ring CC stretching (ν_{8a}), and the in-plane ring breathing (ν_{12}) modes of DMPI, respectively. One can notice at first glance that the spectral peaks in Figure 2b−c can be correlated with those in Figure 2a. This implies that the species responsible for Figure 2b−c are DMPI presenting on Au and Pt nanoaggregates, respectively. The observation of SERS spectrum from an Au nanoaggregate film is not unusual, but it is remarkable that a high-quality SERS spectrum can also be obtained from a Pt nanoaggregate film.

A close examination reveals that substantial spectral differences exist, not only between the NR and SERS spectra of DMPI, but also between the two SERS spectra obtained from the Au and Pt nanoaggregate films. When comparing the two spectra in parts a and b of Figure 2, the most noticeable differences are associated with the NC stretching band along with the ring CC stretching band (ν_{8a}) and the C−NC stretching band. The ν_{8a} band becomes very intense, while the C−NC band is weakened considerably upon adsorbing on Au nanoaggregates. In addition, the C−NC stretching peak is shifted by as much as 18 cm^{-1}, while the ν_{8a} peak is shifted only by 3 cm^{-1}. The more remarkable thing is that the NC stretching peak is shifted from 2123 to 2170 cm^{-1} upon adsorbing on Au nanoaggregates. That is, the NC stretching peak is blue-shifted by as much as 47 cm^{-1}. In addition, the NC stretching band is broadened considerably, viz. from 5 to 20 cm^{-1}, by the surface adsorption on Au, whereas the ring-associated bands including ν_{8a} are broadened at best by 2 cm^{-1}. The substantial blue-shift of the NC stretching mode can be understood by invoking the fact that the carbon lone-pair electrons in the isocyanide group have an antibonding character. The donation of these electrons to gold should increase the strength of the NC bond. The substantial band broadening is associated with the vibrational energy relaxation channel provided by the direct contact of the NC group with the metal substrate. All of these spectral characteristics indicate that DMPI must adsorb on Au exclusively by forming an Au−CN bond. A similar conclusion was made for other isocyanides self-assembled, not only on powdered Au,[17] but also on colloidal Au surfaces.[30]

In a similar way to the case of Au surface adsorption, the ν_{8a} band is strongly intensified, and the C−NC band is in turn considerably weakened when adsorbing on Pt nanoaggregates. The amounts of peak shift of these modes are also comparable to those found on Au. Otherwise, the peak positions, as well as the bandwidths, of the ring-associated modes in Figure 2c are comparable to those in Figure 2a. A dramatic spectral difference is found, however, in the NC stretching region. As can be seen in Figure 2c, three bands appear at 2166, 2124, and 1997 cm^{-1} when DMPI is adsorbing on Pt nanoaggregates; the peak positions are determined by Lorentzian fitting. This is in contrast with the observation of Horswell et al.[31] that only one NC stretching band appears at 2218 cm^{-1} in the FTIR spectrum of dodecylisocyanide-coated Pt nanoparticles; the observed frequency is ~70 cm^{-1} higher than that of free dodecylisocyanide. The highest NC stretching frequency, 2166 cm^{-1}, in Figure 2c is in fact comparable to that found for DMPI on Au; the NC stretching mode has thus blue-shifted by ~40 cm^{-1} in this case. The other frequency, 2124 cm^{-1}, in Figure 2c is close to that of neat DMPI, while another frequency, 1997 cm^{-1}, is lower by as much as 126 cm^{-1} than that of neat DMPI. We assume that these three bands have nothing to do with any overtone or combination bands of lower frequency modes. We, rather, attribute those three bands to the three different binding sites on Pt from which they arise. Accordingly, we presume that DMPI also adsorbs on Pt exclusively by forming a Pt−CN bond.

As mentioned already, the negligible peak shift, i.e., from 1593 to 1590 cm^{-1}, as well as the insignificant band broadening of the ring breathing mode (ν_{8a}), i.e., from 6 to 8 cm^{-1}, dictate that the possibility of a direct ring π orbital-to-metal interaction is quite low. According to the electromagnetic theory of SERS, vibrational modes directed along the surface normal should be enhanced more than the parallel ones.[3] The strong enhancement of the ν_{8a} band in Figure 2b−c can be understood on this ground to imply that DMPI takes a vertical stance with respect to the Au and Pt surfaces. The weakness of the out-of-plane bands at 497 and 463 cm^{-1} in the surface spectra is also in conformity with the vertical orientation of DMPI. The fact that the benzene ring CH stretching band is identified, although weak, at ~3060 cm^{-1} in Figure 2b−c is another indication that DMPI assumes a vertical orientation on both the Au and Pt surfaces.

Isocyanides are isoelectronic with carbon monoxide and are considered to bind to metals in a similar manner. The lower NC frequency would then be attributed to the metal-to-adsorbate π back-bonding because the latter type of bonding was known

to become more prevalent when CO was adsorbing in sequence on on-top, 2-fold bridge, and 3-fold hollow sites of Au or Pt. Recently, Blizanac et al.[32] reported that the CO stretching peak could appear in the ranges of 2115−2140 cm^{-1}, 2005−2070 cm^{-1}, or 1940−1990 cm^{-1}, in accordance with the adsorption on the on-top, 2-fold bridge, and 3-fold hollow sites of Au, respectively. Similar multiple CO stretching bands have been observed for a long time for CO adsorbed on various transition metals, including Pt.[33−37] Intuitively, one may assume that the adsorption of cyanide is more similar than CO to that of DMPI on Pt. By then invoking that usually a π interaction is much weaker than a σ interaction for CN^-,[38,39] while a π interaction is as important as a σ interaction for CO, the multiple NC stretching bands observed herein may have nothing to do with the π back-donation. However, according to the theoretical work of Guy et al.,[40] aryl isocyanide can also be a good π acceptor. Thus, it may not be unusual to observe multiple NC stretching peaks due to π back-donation from Pt. We nonetheless could not identify multiple peaks for DMPI adsorbed on Au nanoaggregates. The reason for the absence of multiple NC stretching bands in this system is unclear. We simply note that the density of states of Pt at its Fermi level is substantially different from that of Au. Probably, the Pt surface is contributed more by d-electrons than the Au surface, so that the π back-donation will occur more favorably on Pt than on Au.

The intensity ratio of the three NC stretching peaks at 2166, 2124, and 1997 cm^{-1} in Figure 2c is determined to be ∼3:14:1 (see the inset; the band areas were also determined by Lorentzian fitting). The fact that the peak at 2124 cm^{-1} is 5−10 times stronger than the other two peaks may indicate that the 2-fold bridge site is energetically more favorable than the on-top and the 3-fold hollow sites for the adsorption of DMPI on Pt nanoaggregates. According to the literature data, CO should adsorb on Pt (111) occupying both the on-top and the 2-fold bridge sites, while only the on-top site is preferred when adsorbing on Pt (100) and Pt (110) planes. These data may indicate that the 3-fold hollow site is energetically less favorable than the on-top and bridge sites. As can be seen in Figure 1d, the Pt nanoaggregate films in this work were composed mostly of (111) planes; next strong peaks were due to (200) and (220) reflections, but the (100) and (110) reflection peaks were not observed at all. The prominent appearance of the NC stretching peak at 2124 cm^{-1} in Figure 2c may then be associated with the abundance of (111) planes at Pt nanoaggregates.

Electrochemical Potential Dependence of DMPI on Au and Pt. Because we were able to obtain high-quality SERS spectra of DMPI on Au and Pt in ambient conditions, it was also expected to be possible to obtain high-quality SERS spectra in an electrochemical environment. In fact, potential-dependent SERS spectra were reproducibly obtained, not only from the Au electrode, but also from the Pt electrode, specifically in the potential region between +0.2 and −0.6 V vs a Ag/AgCl reference electrode in 0.1 M $NaClO_4$ aqueous solution. This can be evidenced from parts a and b of Figure 3 that show, respectively, the potential-dependent SERS spectra of DMPI on Au and Pt electrodes. Much the same spectra are also obtained in 0.01 and 0.001 M $NaClO_4$ solutions. (We should mention that the SERS spectral pattern was not restored, however, once the potential was swept outside the region −0.8 to approximately +0.4 V. The reason is not yet known. The morphology of the electrode surface seemed not to be affected by the potential variation because the SERS activity was invariant, even after excursion to +0.5 V, as well as to −1.0 V, for 10 min. We nonetheless confirmed that DMPI was irreversibly desorbed from the metal electrodes when the potential was lowered below −0.8 V.)

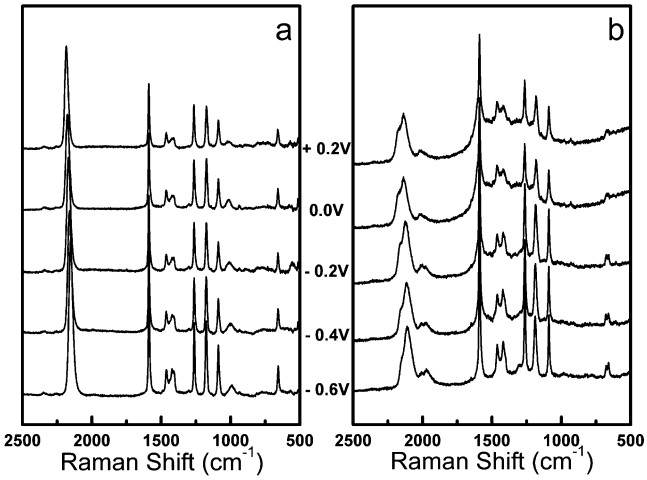

Figure 3. Potential-dependent SERS spectra of DMPI adsorbed on (a) Au and (b) Pt nanoaggregate films recorded at −0.6, −0.4, −0.2, 0.0, +0.2 V vs Ag/AgCl reference electrode in 0.1 M $NaClO_4$ aqueous solution. All the spectra were measured by using a He/Ne laser at 632.8 nm with the acquisition time of 90 s.

The SERS spectral patterns in Figure 3 are seen to vary little upon changes in the surface potential. Specifically, the peak positions, as well as the bandwidths of the ring modes, are not subjected to change following the potential variation. The relative peak intensities of the ring modes are also invariant with respect to the potential variation. This may indicate that the perpendicular orientation of DMPI is maintained on both electrodes irrespective of the potential variation. However, the absolute peak intensities of the ring modes are observed to decrease slightly upon increasing the electrode potential. This may be due to the involvement of the chemical enhancement mechanism of SERS in these electrochemical systems.[41]

In contrast with the ring modes, noticeable peak shifts are observed for the NC stretching bands, not only on Au, but also on a Pt electrode. In Figure 3, all the NC stretching peaks are gradually blue-shifted following the increase in the surface potential. This can be understood by referring to the bonding scheme of DMPI to Au and Pt mentioned above. As the potential is made more positive, there is increased σ donation from the C atom to the metal, resulting in a greater shift of electron density from the N atom into the NC bond, and as a consequence, the bond order and the vibrational frequency are increased. The opposite will take place when the potential is made more negative. It has also to be considered that back-donation from the metal to the NC π^* orbitals can occur at negative potentials, decreasing the bond order and vibrational frequency. In fact, for DMPI adsorbed on Au, the NC stretching peaks are observed at 2182, 2175, 2167, 2160, and 2153 cm^{-1} at 0.2, 0.0, −0.2, −0.4, and −0.6 V, respectively. As can be seen in Figure 4a, these values vary linearly with a slope of ∼38 cm^{-1}/V. The NC stretching frequencies observed herein are all much higher than that of free isocyanide. This suggests that, even at negative potentials, back-bonding makes only a minor contribution to the spectral feature of DMPI assembled on Au nanoaggregates. A similar observation was made by Horswell et al.[25] in their SNIFTIRS study of a 1,8-diisocyanooctane derivatized Au electrode; the potential dependence of the NC stretching frequency was 30 cm^{-1}/V in that case.

For DMPI adsorbed at the on-top site of the Pt nanoaggregates, the NC stretching peak is observed at 2176, 2171, 2163, 2156, and 2148 cm^{-1} at 0.2, 0.0, −0.2, −0.4, and −0.6 V,

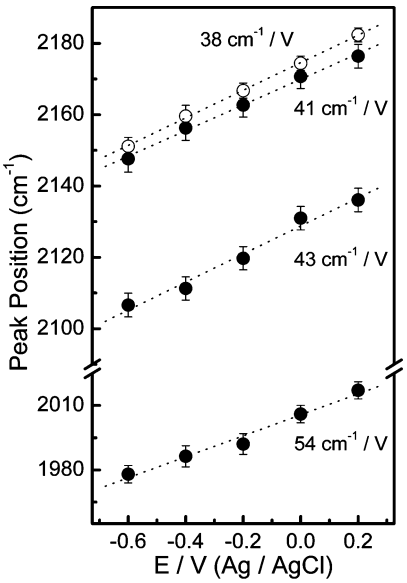

Figure 4. NC stretching frequency vs electrode potential drawn for DMPI on (a) Au nanoaggregates (open circle) and (b−d) Pt nanoaggregates (closed circle); (b), (c), and (d) correspond, respectively, to three peaks at 2166, 2124, and 1997 cm^{-1} in the inset of Figure 2c. See text.

respectively. As can be seen in Figure 4b, these values also vary linearly with a slope of ~41 cm^{-1}/V. Once again, the frequencies at negative potentials are higher than that of free isocyanide, implying that the π back-bonding is not important for DMPI adsorbed on the on-top site of the Pt substrate. This may reflect the fact that the acceptor orbital of organic isocyanides has a higher energy, which is unfavorable for π back-bonding.

For DMPI adsorbed at the 2-fold bridge site of the Pt nanoaggregates, the NC stretching peak is observed at 2136, 2131, 2120, 2111, and 2106 cm^{-1} at 0.2, 0.0, −0.2, −0.4, and −0.6 V, respectively. As can be seen in Figure 4c, these values vary linearly with a slope of ~43 cm^{-1}/V. The frequencies at negative potentials are clearly lower than that of free isocyanide, and this has to be attributed to the back-donation from the metal. As can be seen in Figure 4d, the NC stretching peak for DMPI adsorbed at the 3-fold hollow sites also varies linearly with a slope of ~54 cm^{-1}/V. In this case, the π back-bonding must be more important than the σ donation from the C atom to the metal. Herein, also we have to mention that the intensity ratio of 3:14:1, seen in Figure 2c, of the three NC stretching peaks at 2166, 2124, and 1997 cm^{-1}, obtained in ambient conditions, is maintained even in Figure 3b, obtained in an electrochemical environment. This may indicate that the adlayer structure of DMPI on Pt nanoaggregates in the electrochemical environment is barely different from that in ambient conditions.

The potential-dependent frequency change observed herein for DMPI is comparable to the value determined by infrared spectroscopy for CO adsorbed on Pt in acidic electrolytes at constant coverage.[33] For CO adsorbed on metals, this has been explained by either the electrochemical Stark effect or by the bonding characteristics of CO derived from molecular orbital theory.[42,43] Stark tuning originates from the interaction of the polar adsorbate with the interfacial electric field. As mentioned already, the potential-dependent SERS spectral pattern of DMPI was nearly invariant at least in 0.1, 0.01, and 0.001 M $NaClO_4$ solutions. This may be understood by presuming that the isocyanide group probed by Raman spectroscopy is present well inside the double-layer region due to the close-packed assembly of DMPI on the nanoaggregate films; the close-packed DMPI monolayer can then form a barrier at which the aqueous double-layer forms. In that case, the potential decay within the DMPI layer will be linear, although a significant fraction of the applied potential may reach the aqueous region. The Stark effect, if it exists, is then expected to be largely independent of the electrolyte concentration. In any case, we suppose that the electrochemical Stark effect is minor, compared to the bonding effect, for the occurrence of the potential-dependent frequency change for DMPI. According to a recent study of mixed monolayers composed of 12-mercaptododecanenitrile and 7-heptanethiol on the Ag surface, the Stark tuning rate is in fact at best 10 cm^{-1}/V for the nitrile stretching mode.[44]

4. Summary and Conclusion

The adsorption characteristics of 2,6-dimethylphenylisocyanide (DMPI) on Au and Pt surfaces have been investigated by means of electrochemical potential-dependent surface-enhanced Raman scattering (SERS) spectroscopy. First of all, we confirmed that Pt nanoaggregate films are efficient SERS-active substrates. SERS spectra clearly illustrated that DMPI should adsorb, not only on Au, but also on Pt nanoaggregates exclusively by forming a metal−CN bond, assuming a vertical orientation with respect to the metal substrate. The detailed bonding scheme on Au seemed, however, different from that on Pt. On the Au surface, DMPI appeared to adsorb mostly on the on-top site. In contrast, on Pt, DMPI seemed to adsorb, not only on the on-top site, but also on the 2-fold bridge and 3-fold hollow sites. These apparently different adsorption schemes are presumed to be due to the presence of comparatively larger d-electrons at the Pt surface than at the Au surface. From the potential-dependent SERS, the adsorbate orientation was found not to change, at least in the potential range of +0.2 to −0.6 V vs the Ag/AgCl reference electrode, although the bond order of the isocyanide group could be varied linearly against the electrode potential. The latter characteristics may imply that the Au−CN and Pt−CN combinations would be an ideal couple when designing molecular-scale wires. At any rate, the accessibility of SERS-active Pt nanoaggregate films in an electrochemical environment is believed to make a tremendous impact on the development and advancement of electrochemical catalysis.

Acknowledgment. This work was supported by the Korea Research Foundation (KRF, 2003-015-C00285).

References and Notes

(1) Han, S. H.; Seo, H.; Chung, Y. K.; Kim, K. *Langmuir* **2000**, *16*, 9493.
(2) Bin, X.; Zawisza, I.; Goddard, J. D.; Lipkowski, J. *Langmuir* **2005**, *21*, 330.
(3) Moskovits, M. *Rev. Mod. Phys.* **1985**, *7*, 209.
(4) Chang, R. K.; Furtak. T. E. *Surface Enhanced Raman Scattering*; Plenum Press: New York, 1982.
(5) Park, S.; Yang, P.; Corredor, P.; Weaver, M. J. *J. Am. Chem. Soc.* **2002**, *124*, 2428.
(6) Tian, Z. Q.; Ren, B.; Wu, D. T. *J. Phys. Chem. B* **2002**, *106*, 9463.
(7) Kim, N. H.; Kim, K. *Chem. Phys. Lett.* **2004**, *393*, 478.
(8) Joachim, C.; Gimzewski, J. K.; Aviram, A. *Nature* **2000**, *408*, 541.
(9) Tour, J. M. *Acc. Chem. Res.* **2000**, *33*, 791.
(10) Seminario, J. M.; De La Cruz, C. E.; Derosa, P. A. *J. Am. Chem. Soc.* **2001**, *123*, 5616.
(11) Samanta, M. P.; Tian, W.; Datta, S.; Henderson, J. I.; Kubiak, C. P. *Phys. Rev. B* **1996**, *53*, 7626.
(12) Chen, J.; Reed, M. A.; Rawlett, A. M.; Tour, J. M. *Science* **1999**, *286*, 1550.
(13) Yaliraki, S. N.; Kemp, M.; Ratner, M. A. *J. Am. Chem. Soc.* **1999**, *121*, 3428.

(14) Hickman, J. J.; Laibinis, P. E.; Auerbach, D. I.; Zou, C.; Gardner, T. J.; Whiteside, G. M.; Wrighton, M. S. *Langmuir* **1992**, *8*, 357.
(15) Robertson, M. J.; Angelici, R. J. *Langmuir* **1994**, *10*, 1488.
(16) Henderson, J. I.; Feng, S.; Ferrence, G. M.; Bein, T.; Kubiak, C. P. *Inorg. Chim. Acta* **1996**, *242*, 115.
(17) Ontko, A. C.; Angelici, R. J. *Langmuir* **1998**, *14*, 1684.
(18) Lin, S.; McCarley, R. L. *Langmuir* **1999**, *15*, 151.
(19) Han, H. S.; Han, S. W.; Joo, S. W.; Kim, K. *Langmuir* **1999**, *15*, 6868.
(20) Murphy, K.; Azad, S.; Bennett, D. W.; Tysoe, W. T. *Surf. Sci.* **2001**, *467*, 1.
(21) Clot, O.; Wolf, M. O. *Langmuir* **1999**, *15*, 8549.
(22) Huc, V.; Bourgoin, J. P.; Bureau, C.; Valin, F.; Zalczer, G.; Palacin, S. *J. Phys. Chem. B* **1999**, *103*, 10489.
(23) Ansell, M. A.; Cogan, E. B.; Pages, C. J. *Langmuir* **2000**, *16*, 1172.
(24) Henderson, J. I.; Feng, S.; Bein, T.; Kubiak, C. P. *Langmuir* **2000**, *16*, 6183.
(25) Horswell, S. L.; O'Neil, I. A.; Schiffirin, D. J. *J. Phys. Chem. B* **2001**, *105*, 941.
(26) Chen, J.; Calvet, L. C.; Reed, M. A.; Carr, D. W.; Grubisha, D. S.; Bennett, D. W. *Chem. Phys. Lett.* **1999**, *313*, 741.
(27) Lee, I.; Han, S. W.; Kim, K. *J. Raman Spectrosc.* **2001**, *32*, 1732.
(28) Kim, N. H.; Kim, K. *J. Raman Spectrosc.* **2005**, *36*, 623.
(29) Joo, S.-W.; Kim, W.-J.; Yun, W. S.; Hwang, S.; Choi, I. S. *Appl. Spectrosc.* **2004**, *58*, 218.
(30) Kim, H. S.; Lee, S. J.; Kim, N. H.; Yoon, J. K.; Park, H. K.; Kim, K. *Langmuir* **2003**, *19*, 6701.
(31) Horswell, S. L.; Kiely, C. J.; O'Neil, I. A.; Schiffrin, D. J. *J. Am. Chem. Soc.* **1999**, *121*, 5573.
(32) Blizanac, B. B.; Arenz, M.; Ross, P. N.; Markoviæ, N. M. *J. Am. Chem. Soc.* **2004**, *126*, 10130.
(33) Morkel, M.; Unterhalt, H.; Klüner, T.; Rupprechter, G.; Freund, H. J. *Surf. Sci.* **2005**, *586*, 146.
(34) Borguet, E.; Dai, H. L. *J. Phys. Chem. B* **2005**, *109*, 8509.
(35) Grossmann, A.; Erley, W.; Ibach, H. *Surf. Sci.* **1996**, *355*, L331.
(36) Ren, B.; Lin, X.; Yan, J.; Mao, B.; Tian, Z. *J. Phys. Chem. B* **2003**, *101*, 1338.
(37) Gómez, R.; Pérez, J. M.; Gullón, J. S.; Montiel, V.; Aldaz, A. *J. Phys. Chem. B* **2004**, *108*, 9943.
(38) Ample, F.; Curulla, D.; Fuster, F.; Clotet, A.; Ricart, J. M. *Surf. Sci.* **2002**, *497*, 139.
(39) Daum, W.; Dederichs, F.; Müller, J. E. *Phys. Rev. Lett.* **1998**, *80*, 766.
(40) Guy, M. P.; Guy, J. T.; Bennett, D. W. *J. Mol. Struct. THEOCHEM* **1985**, *122*, 95.
(41) Lombardi, J. R.; Birke, R. L.; Sanchez, L. A.; Bernard, I.; Sun, S. C. *Chem. Phys. Lett.* **1984**, *104*, 240.
(42) Korzeniewski, C.; Shirts, R. B.; Pons, S. *J. Phys. Chem.* **1985**, *89*, 2297.
(43) Zou, S.; Weaver, M. J. *J. Phys. Chem.* **1996**, *100*, 4237.
(44) Oklejas, V.; Sjostrom, C.; Haris, J. M. *J. Am. Chem. Soc.* **2002**, *124*, 2408.